Inorganic Chemistry

Article

pubs.acs.org/IC

# $Sr_3BeB_6O_{13}$: A New Borate in the SrO/BeO/$B_2O_3$ System with Novel Tri-Six-Membered Ring $(BeB_6O_{15})^{10-}$ Building Block

Wenjiao Yao,[†,§] Hongwei Huang,[‡] Jiyong Yao,[†] Tao Xu,[†,§] Xingxing Jiang,[†,§] Zheshuai Lin,*[,†] and Chuangtian Chen[†]

[†]Beijing Center for Crystal R&D, Key Laboratory of Functional Crystals and Laser Technology of the Chinese Academy of Sciences, Technical Institute of Physics and Chemistry, Chinese Academy of Sciences, Beijing 100190, PR China

[‡]School of Materials Science and Technology, China University of Geosciences, Beijing 100083, PR China

[§]University of the Chinese Academy of Sciences, Beijing 100049, PR China

Supporting Information

**ABSTRACT:** A new polyborate $Sr_3BeB_6O_{13}$ has been synthesized and grown by the traditional solid-state reaction method and spontaneous crystallization flux method. It crystallizes in orthorhombic space group *Pnma* (No. 62) with the following unit cell dimensions: $a$ = 12.775(3) Å, $b$ = 10.029(2) Å, $c$ = 8.0453(16) Å, and $Z$ = 4. The crystal is characterized by an infinite two-dimensional network with a tri-six-membered ring $(BeB_5O_{13})^{9-}$ anionic group, which was first found in beryllium borates. Ultraviolet (UV)−visible−near-infrared diffuse reflectance spectroscopy demonstrates that its UV cutoff edge is below 200 nm, and the first-principles electronic structure calculations reveal its energy band gap of 7.03 eV (~175 nm). Thermal analysis exposes its incongruent feature at 1043 °C. IR spectroscopy measurements are consistent with the crystallographic study. These data reveal that this crystal would be applied as a deep-ultraviolet optical material.

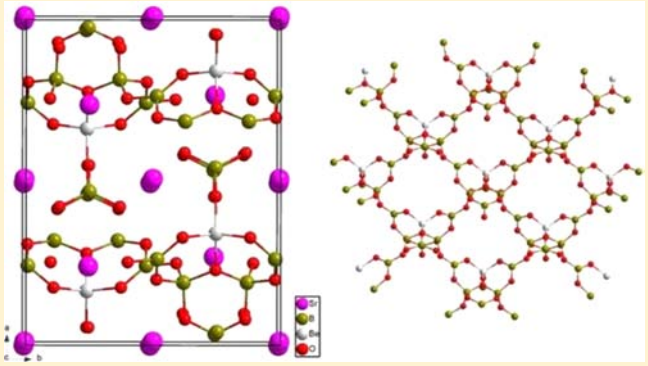

## INTRODUCTION

Borates have been attracted continuous interest for nearly four decades. The main reason lies in their rich structural chemistry and increasing demand in nonlinear optics, birefringent optics, and electrode materials.[1−3] The boron atom can be either three- or four-coordinated by oxygen atoms to form a $BO_3$ triangle or a $BO_4$ tetrahedron, respectively, which can further link together to form numerous polymeric (chain, layer, and network) or isolated (island) anions with no internal degrees of freedom by sharing corners and edges. $[B_3O_6]^{6-}$ in $\beta$-$BaB_2O_4$ (BBO),[4] $[B_3O_7]^{5-}$ in $LiB_3O_5$ (LBO),[5] and $[B_6O_{10}]^{2-}$ in $K_3B_6O_{10}Cl$[6] are typical examples. In addition, the incorporation of Be/Al/Si/P−O/F polyhedrons further expands the structural diversity of borates to a great extent.[7] In particular, beryllium borates have played an important role in deep-ultraviolet (deep-UV) optical crystals,[8−10] because they possess a very large energy gap as long as the A-site cations are alkali or alkaline earth metals.[11] The intensive study of the R-BeO-$B_2O_3$ system (R is alkali oxide/fluoride or alkaline earth oxide/fluoride) has given rise to the discovery of more than 10 compounds, such as $KBe_2BO_3F_2$ (KBBF), the sole deep-UV nonlinear optical (NLO) crystal for the practical generation of coherent 177.3 nm light,[12] and the $NaBeB_3O_6$ (NBBO) family,[13] the promising candidates for 193 nm harmonic generation.

In the SrO/BeO/$B_2O_3$ system, only two compounds have been reported, namely, $SrBe_2(BO_3)_2$[14] and $Sr_2Be_2B_2O_7$.[15] Both of them are layered constructs, $[Be_2(BO_3)_2]^{2-}$ for the former and $[Be_3B_3O_9]^{9-}$ for the latter, and they share the same Be:B ratio, i.e., 1:1. We propose that further modifications of the Be:B ratio might lead to new structures instead of the strongly layered ones in the known compounds.

Under this consideration, in this work, experimental investigations of the SrO/BeO/$B_2O_3$ ternary system have been conducted to explore the large energy gap crystals containing new beryllium borate anionic groups or frameworks. A new $Sr_3BeB_6O_{13}$ compound with the novel tri-six-membered ring $(BeB_6O_{15})^{10-}$ building block was successfully discovered. The synthesis, crystal structure, and optical and thermal properties of $Sr_3BeB_6O_{13}$ are reported.

## EXPERIMENTAL SECTION

**Synthesis and Crystal Growth.** $SrCO_3$ (AR), BeO (99.5%), $H_3BO_3$ (AR), $B_2O_3$ (99.5%), NaF (AR), and LiF (AR) from commercial sources were used as received. Polycrystalline samples were obtained by traditional solid-state reaction with a stoichiometric mixture of $SrCO_3$, BeO, and $H_3BO_3$. Because of the toxicity of BeO, all of the experiments

Received: March 1, 2013
Published: May 3, 2013

   dx.doi.org/10.1021/ic400515m | Inorg. Chem. 2013, 52, 6136−6141

were performed in a ventilated system. The raw materials were carefully ground and mixed in an agate mortar and packed into a platinum crucible; the materials were then heated in a muffle furnace to ~600 K in the first round to ensure the decomposition of $H_3BO_3$ and $SrCO_3$. The mixture was ground adequately and heated gradually to 1253 K over 6 days with several grindings in that interval and powder X-ray diffraction (PXRD) analysis until the monophasic powders with white color were achieved. The chemical equation can be expressed as follows:

$$3SrCO_3 + BeO + 6H_3BO_3 \rightarrow Sr_3BeB_6O_{13} + 3CO_2 + 9H_2O$$

The $Sr_3BeB_6O_{13}$ single crystal was obtained by the flux method through spontaneous crystallization using $B_2O_3$ and NaF (or LiF) as flux. The synthetic samples and flux at appropriate proportions were homogeneously mixed, placed in a platinum crucible, and gradually heated in a self-made furnace until they melted. The melted samples were kept at that temperature for at least 24 h to ensure homogeneity. The temperature was then lowered at a rate of 10 K/day until the mixture was curdled. The crucible was then taken out of the furnace and cooled to room temperature in air. Many colorless, transparent block crystals were obtained for later tests. The temperature was stabilized with a precision of 0.1 K.

**Structural Determination.** Single-crystal X-ray diffraction data for $Sr_3BeB_6O_{13}$ were collected at room temperature (293 K) on a Rigaku AFC10 single-crystal diffractometer with graphite-monochromatic Mo K$\alpha$ radiation ($\lambda$ = 0.71073 Å) and a Saturn CCD detector. A colorless, transparent crystal with dimensions of 0.25 mm × 0.18 mm × 0.15 mm was selected for structure determination. Crystalclear was used to record the intensity data and to perform cell refinement and data reduction. The structure was determined with Shelxtl-97[16] by the direct method and refined by full-matrix least-squares techniques with anisotropic thermal parameters. The crystal data and structural refinement for $Sr_3BeB_6O_{13}$ are presented in Table 1. The atomic coordinates and calculated band valence sum (BVS) are summarized in Table 2 (the related anisotropic displacement parameters are listed in Table S1 of the Supporting Information).

**Table 1. Crystallographic Data for $Sr_3BeB_6O_{13}$**

| | |
|---|---|
| formula | $Sr_3BeB_6O_{13}$ |
| formula weight (g/mol) | 544.73 |
| crystal system | orthorhombic |
| space group | *Pnma* (No. 62) |
| unit cell parameters | $a$ = 12.775(3) Å |
| | $b$ = 10.0293(29) Å |
| | $c$ = 8.0453(16) Å |
| | $V$ = 1030.77(38) Å$^3$ |
| | $Z$ = 4 |
| index ranges | $-17 \le h \le 18$ |
| | $-12 \le k \le 14$ |
| | $-11 \le l \le 11$ |
| $d_{calc}$ (g/cm$^3$) | 3.510 |
| $\theta$ range (deg) | 2.5317−31.4867 |
| no. of reflections | 1799 |
| no. of refined parameters | 116 |
| $R$ indices (all data) | 0.0277/0.0510 |
| final R indices [$I > 2\sigma(I)$] | 0.0229/0.0497 |
| goodness of fit on $F^2$ | 1.198 |
| extinction coefficient | 0.0086(3) |

Inductively coupled plasma optical emission spectrometry (ICP-OES) was also conducted to determine the composition of the crystal. The test was performed on a Varian 710-ES instrument with Sepex Certiprep standards, which reveals a Be:B:Sr ratio of 1:5.8918:2.9857.

**X-ray Powder Diffraction.** The powder X-ray diffraction (PXRD) investigation was conducted on the finely ground polycrystallines with a Bruker D8 advanced X-ray diffractometer using Cu Ka radiation ($\lambda$ = 1.5418 Å). The powder diffraction pattern was recorded in the angular range from 7° to 80° with a scanning step width of 0.02° and a rate of 0.2°/s. Theoretical simulation were also conducted on the basis of single-crystal crystallographic data.

**Thermal Analysis [differential scanning calorimetry (DSC)].** DSC measurements were taken with ground crystals of the title compound using a Labsys TG-DTA16 (SETARAM) thermal analyzer calibrated with $Al_2O_3$. A sample (~10 mg) of ground crystal was placed in a platinum crucible and heated from room temperature to 1250 °C at a rate of 10 °C/min in a nitrogen atmosphere. The melted residues were examined and analyzed by X-ray powder diffraction after the experiments.

**IR Spectroscopy.** IR spectroscopy was conducted with the objective of specifying and comparing the coordination of boron in the title compound. The mid-infrared spectrum was obtained at room temperature via a Bio-Rad FTS-60 FTIR spectrometer. The sample (5 mg) and dried KBr (500 mg) were mixed thoroughly together. The spectroscopic data were collected in a range from 400 to 4000 cm$^{-1}$ with a resolution of 1 cm$^{-1}$.

**UV−Visible−Near-Infrared (NIR) Diffuse Reflectance Spectroscopy.** UV−visible−NIR diffuse reflectance data for the title compound were collected with a SolidSpec-3700 DUV spectrophotometer in the wavelength range from 200 to 2600 nm. Fluororesin was applied as the standard.

**First-Principles Calculations.** The electronic structure calculations were performed with CASTEP,[17] a plane-wave pseudopotential total energy package based on density functional theory.[18] The optimized norm-conserving pseudopotential[19] in Kleiman−Bylander[20] form for Sr, Be, B, and O allows us to use a small plane basis set without compromising the accuracy required by the calculation. A kinetic energy cutoff of 800 eV and a Monkhorst-pack $k$-point mesh[21] with a density of (1 × 1 × 2) points in the Brillouin zone were chosen. The convergence tests showed that these calculation parameters are adequate for this study. Our previous first-principles studies[22] revealed that in the UV borates the band gaps can be accurately predicted by the hybrid exchange correlation PBE0 functionals,[23] while the dispersion of band structures can be reproduced well by generalized gradient approximation (GGA).[24] Therefore, the difference between the PBE0 and GGA band gaps is used as the scissors operator[25] to shift the conduction bands in the GGA electronic structures. By this treatment, the electronic structure in $Sr_3BeB_6O_{13}$ can be correctly determined.

## RESULTS AND DISCUSSION

**Crystal Structure.** The structure of the title crystal is depicted in Figure 1. It crystallizes in the orthorhombic system in the centrosymmetric *Pnma* space group. In the symmetric unit, Sr, Be, B, and O occupy two, one, four, and eight crystallographically unique positions, respectively. The structure is characterized by the $[BeB_6O_{15}]_\infty$ network composed of a two-dimensional $[BeB_5O_{13}]^{6-}$ framework in the $b$−$c$ plane and interlayer $BO_3$ groups, and the $Sr^{2+}$ ions are located in the cavities coordinated by either eight or nine O atoms (see Figure S1 of the Supporting Information), as depicted in Figure 1a. The adjacent layers are connected by the electrostatic force within the Sr−O polyhedra. Unlike $Sr_2Be_2B_2O_7$ in the SrO/BeO/$B_2O_3$ system, in which the adjacent layers easily glide, twist, or depart from each other, resulting in the polymorphism problem,[27] there are interlayer $BO_3$ groups stretching out from the planar network in $Sr_3BeB_6O_{13}$. Those protruding feelers are inlaid into that from the neighboring layer and further strengthen the linkage between layers. This structural feature is beneficial to growth of the single crystal; the preliminary growth attempts have yielded the $Sr_3BeB_6O_{13}$ single crystals with the size of 3 mm × 3 mm × 3 mm (see Figure 2).

Figure 1b shows the $[BeB_6O_{15}]^{10-}$ basic structural unit. This novel building block consists of one $BeO_4$ tetrahedron, two $BO_4$ tetrahedra, and four triangular $BO_3$ units. The bond lengths and bond angles in the $BeO_4$ tetrahedron range from 1.5733 to 1.7017 Å and from 102.764° to 124.902°, respectively, and in the


dx.doi.org/10.1021/ic400515m | Inorg. Chem. 2013, 52, 6136−6141

**Table 2. Atomic Coordinates and Calculated Bond Valence Sum (BVSs)**

| atom | Wyck. | site | *x*/*a* | *y*/*b* | *c*/*z* | BVS |
|---|---|---|---|---|---|---|
| Sr1 | 4c | m | 0.23798(2) | 1/4 | 0.40536(4) | 2.0893 |
| Sr2 | 8d | 1 | 0.00919(2) | 0.50186(2) | 0.23484(2) | 1.9622 |
| B1 | 8d | 1 | 0.31150(18) | 0.1252(2) | −0.0266(3) | 3.0688 |
| B2 | 8d | 1 | 0.26269(18) | −0.0179(2) | 0.2132(3) | 3.0383 |
| B3 | 4c | m | 0.4717(3) | 1/4 | 0.0641(4) | 3.0037 |
| B4 | 4c | m | 0.0409(3) | 3/4 | 0.0255(4) | 2.8784 |
| Be | 4c | m | 0.1589(3) | 1/4 | 0.7920(5) | 2.0246 |
| O1 | 8d | 1 | 0.25430(11) | 0.09884(15) | 0.12673(19) | 2.2033 |
| O2 | 4c | m | 0.55158(15) | 1/4 | 0.1693(3) | 1.7407 |
| O3 | 8d | 1 | 0.32954(11) | −0.11725(14) | 0.17568(19) | 1.9760 |
| O4 | 8d | 1 | 0.30182(11) | 0.01711(14) | −0.14810(19) | 1.7333 |
| O5 | 8d | 1 | 0.42567(11) | 0.13145(14) | 0.0104(2) | 1.6622 |
| O6 | 4c | m | 0.27264(15) | 1/4 | −0.0979(3) | 1.9754 |
| O7 | 4c | m | −0.04616(16) | 3/4 | 0.1293(3) | 1.5426 |
| O8 | 8d | 1 | 0.08632(11) | 0.62968(14) | −0.01818(19) | 1.8468 |

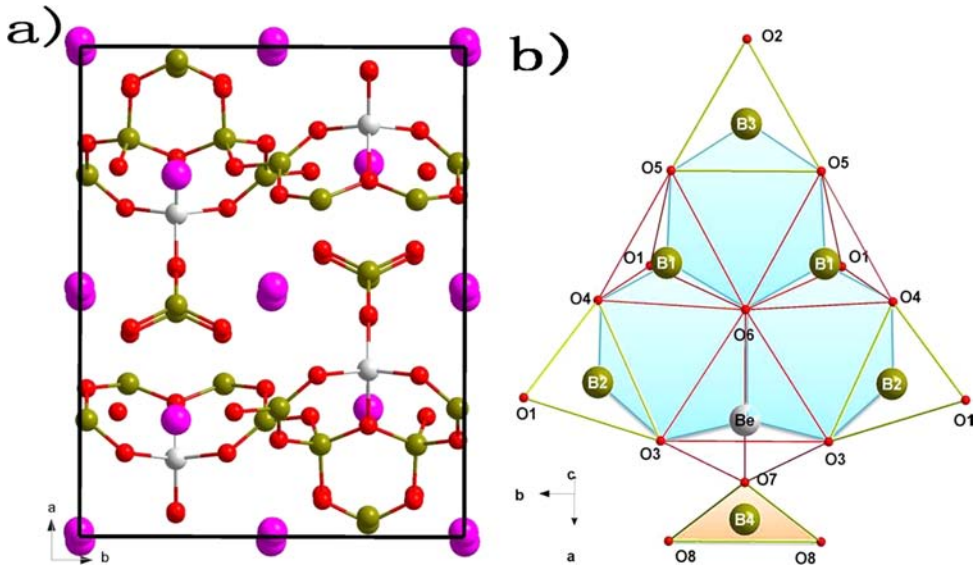


**Figure 1.** Crystal structure of $Sr_3BeB_6O_{13}$. (a) Unit cell (viewed along the *c*-axis). (b) Basic building block $[BeB_6O_{15}]^{10-}$. The Sr, Be, B, and O ions are represented as pink, white, dark yellow, and red spheres, respectively. $BO_4/BeO_4$ tetrahedra and $BO_3$ triangles are drawn as red and green hollow figures, respectively. The interlayer $(BO_3)^{3-}$ and tri-six-membered ring $[BeB_5O_{13}]^{9-}$ are represented by orange and light blue solid profiles, respectively.

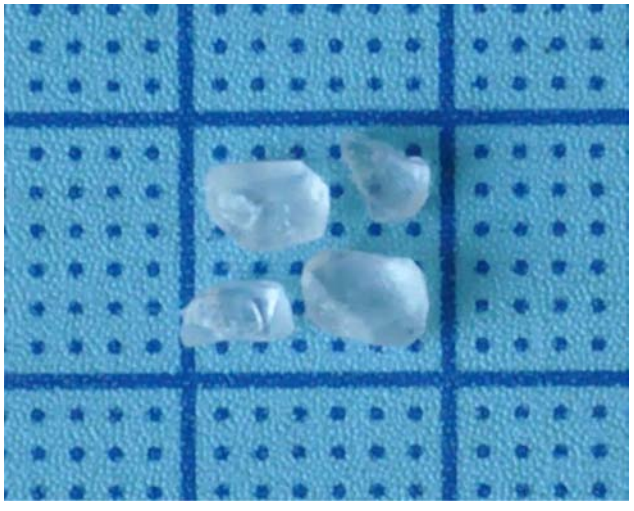

**Figure 2.** Photo of $Sr_3BeB_6O_{13}$ single crystals grown by the flux method.

$BO_4$ tetrahedron from 1.4579 to 1.4899 Å and from 104.305° to 112.837°, respectively. The B−O bond lengths in triangular $BO_3$ vary from 1.3258 to 1.3950 Å, with bond angles from 116.923° to 124.734° (see Table S1 of the Supporting Information). These bond lengths and angles are comparable to those in other beryllium borates.[26] Every two $BO_4/BeO_4$ tetrahedra and one $BO_3$ triangle form a six-membered ring by sharing the corner O atoms. Three rings are further joined together by the common O6 atom, producing a unique tri-six-membered ring configuration, $(BeB_5O_{13})^{9-}$. This tri-six-membered ring is discovered for the first time in the beryllium borates. The interlayer $BO_3$ triangle forms a bridge to the $BeO_4$ tetrahedra through the O7 atom. The $[BeB_6O_{15}]^{10-}$ group belongs to the $C_s$ point group with the mirror plane passing through the Be, B3, B4, O6, and O7 atoms. Each $[BeB_6O_{15}]^{10-}$ group is further linked to its four neighboring counterparts through O1 atoms, forming the framework extending in the *a*−*c* plane.

The six-membered ring has long been observed in borates. One classic representative is commercially used, low-temperature phase $BaB_2O_4$ (BBO),[4] the structure of which contains an


dx.doi.org/10.1021/ic400515m | *Inorg. Chem.* 2013, 52, 6136−6141

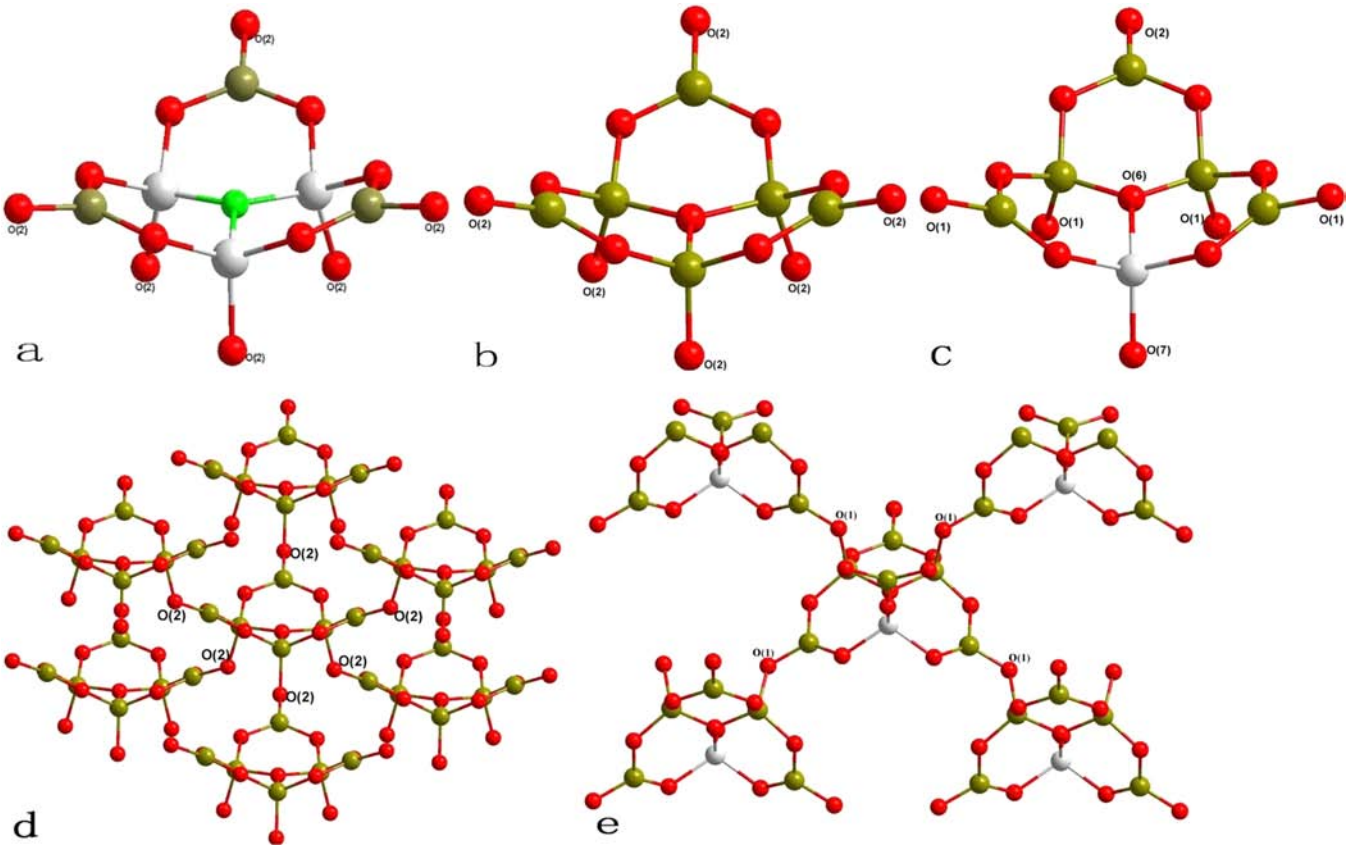


**Figure 3.** (a) $[Be_3B_3O_{12}F]^{10-}$ group in $NaSr_3Be_3B_3O_9F_4$. (b) $[B_6O_{13}]^{8-}$ group in $K_3B_6O_{10}Cl$. (c) $[BeB_5O_{13}]^{9-}$ group in the title crystal. (d) Framework diagram of $K_3B_6O_{10}Cl$ (or $NaSr_3Be_3B_3O_9F_4$). (e) Framework diagram of the title crystal. The Be, B, O, and F ions are represented as white, dark yellow, red, and green spheres, respectively.

isolated $(B_3O_6)^{6-}$ six-membered rings. Later exploration in borates has led to the discovery of double six-membered rings as in $NaBeB_3O_6$ and $ABe_2B_3O_7$ (A = K or Rb),[10] which is highly analogous to a naphthalene molecule. Recently, the tri-six-membered rings, $[Be_3B_3O_{12}F]^{10-}$ and $[B_6O_{13}]^{8-}$ anionic groups (see panels a and b of Figure 3), were discovered in $NaSr_3Be_3B_3O_9F_4$[26] and $K_3B_6O_{10}Cl$,[6] respectively. Actually, these groups have almost the same geometry as the $(BeB_5O_{13})^{9-}$ group (shown in Figure 3c) in the title compound; i.e., all of them exhibit a concave planar configuration with six out-of-ring O atoms stretching to in similar directions. The difference among these three six-membered rings mainly comes from the different constitutional atoms. In addition, the previously found groups possess a 3-fold (C3) axis passing through the center atom and six identical out-of-ring O atoms (O2), which are bridged by the neighbors to construct similar three-dimensional networks, as shown in Figure 3d, and result in the same space group ($R3m$). As a comparison, there are no C3 axis and only four such identical O atoms (O1) in our $[BeB_5O_{13}]^{9-}$ tri-six-membered two-dimensional network, while the other two oxygen atoms are either dangled (O2) or linked to the interlayer $BO_3$ group (O7), as shown in Figure 3e. This is the main crystallographic difference between $Sr_3BeB_6O_{13}$ and the two former compounds.

**Physical Characterization.** The PXRD pattern of the crystalline $Sr_3BeB_6O_{13}$ is compared with the calculated one derived from the single-crystal data, which shows good agreement (see Figure 4a). The PXRD of the synthetic powders by solid-state reaction proves that the pure phase of the compound is obtained. The thermal analysis demonstrates a strong endothermal peak at 1043 °C, as indicated by the DSC curve in Figure 4b. The powder was therefore heated above this temperature, and the PXRD pattern was taken again on the residual. The pattern shows a mixture of glass phases and $SrB_2O_4$, which reveals the incongruent melting compound behavior of the title compound.

IR spectroscopy analysis (Figure 4c) validates the existence of the different borate groups in the crystal structures. The bands in the range of 1396−1232 $cm^{-1}$ correspond to the asymmetric and symmetric stretching vibrations of the triangular borate groups, whereas those in the range of 993−775 $cm^{-1}$ might be attributed to the asymmetric and symmetric stretching vibration modes of tetrahedral borate groups. Peaks at 584 and 673 $cm^{-1}$ are the bending mode of the $BO_3$ group (for detailed peaks, see Table S2 of the Supporting Information). These measurements are consistent with the results for other borates.[28] Figure 4d displays the UV−vis−NIR diffuse reflectance spectroscopy result for $Sr_3BeB_6O_{13}$, which illustrates the high level of transparency in the UV region and cutoff wavelength extending to <200 nm, suggesting the potential of this crystal for UV applications. In addition, the mean refractive index of the $Sr_3BeB_6O_{13}$ crystal is estimated to be 1.716 according to the Lorenz−Lorentz relation.[29]

**Electronic Structure Calculations.** The calculated band gap of $Sr_3BeB_6O_{13}$ is 7.03 eV (~175 nm) and 4.87 eV (~254 nm) by PBE0 and GGA, respectively. Clearly, the PBE0 result is consistent with the experimental value. The band structure shows that $Sr_3BeB_6O_{13}$ is a direct gap crystal. Figure 5 gives the


dx.doi.org/10.1021/ic400515m | Inorg. Chem. 2013, 52, 6136−6141

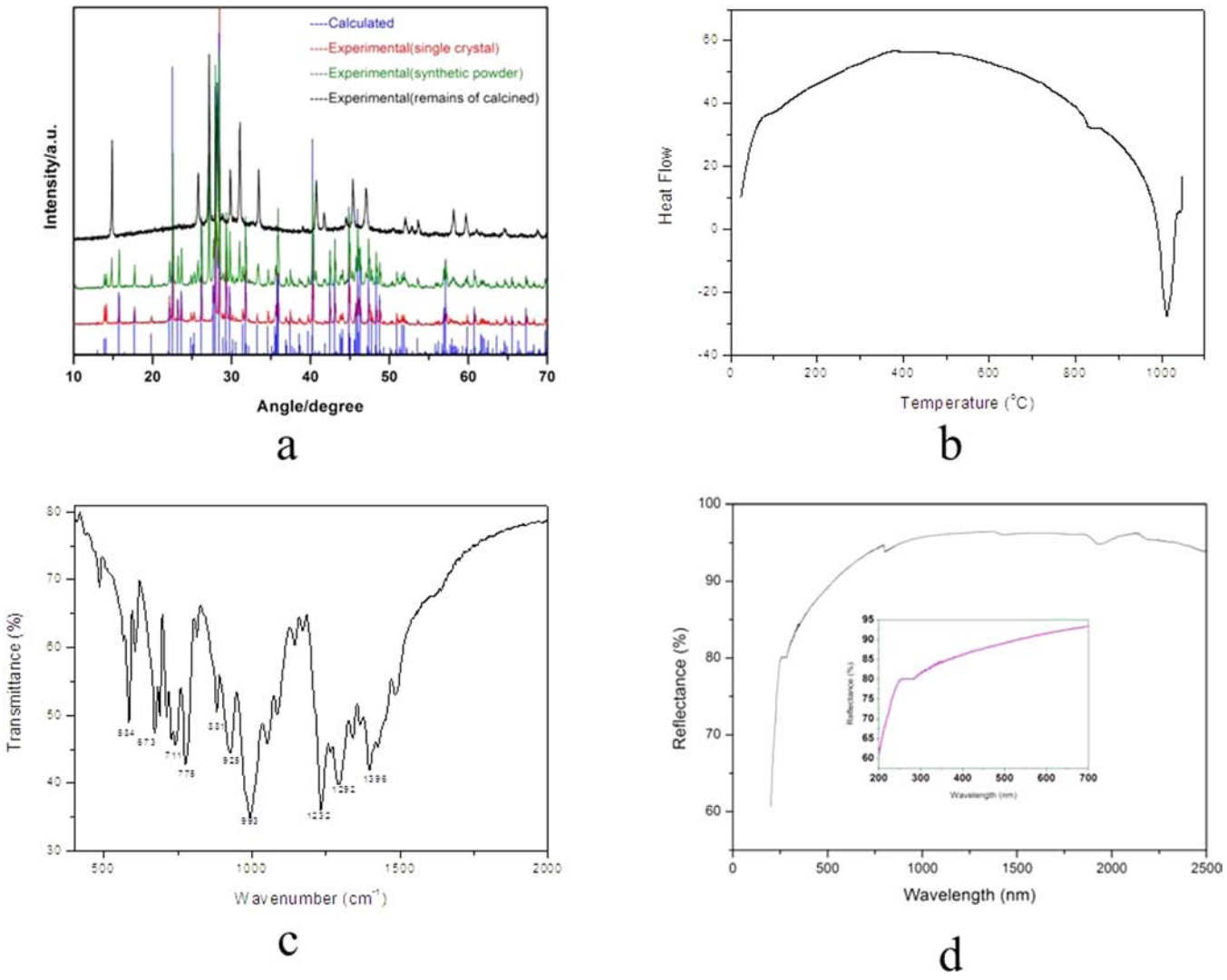


**Figure 4.** Physical characterization of $Sr_3BeB_6O_{13}$: (a) PXRD patterns, (b) DSC curve, (c) IR spectrum, and (d) UV−vis−NIR diffuse reflectance spectroscopy.

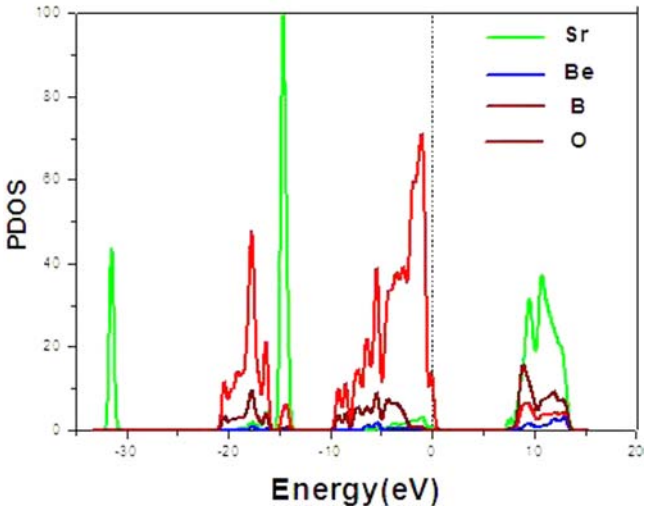


**Figure 5.** Partial density of states (PDOS) of $Sr_3BeB_6O_{13}$.

total density of states (DOS) and partial density of states (PDOS) of the title compound, in which several characteristics can be observed. (1) The Sr 4s and 4p orbitals are strongly localized at −32 and −15 eV, respectively, and do not form chemical bonds with other orbitals. (2) The bands near −17 eV mainly consist of O 2s and B 2p orbitals, revealing the relatively strong hybridization between O and B atoms. (3) Be orbitals have almost no contribution to any of the bands. (4) The upper regions of the valence band (VB) from −10 to 0 eV are mainly composed of O 2p and B 2p orbitals and a fraction of Sr 4d orbitals, suggesting the strong bond between B and O atoms. (5) The bottom of the conduction band (CB) consists of the orbitals from Sr, B, and O, but the contribution from the Sr orbitals is dominant at the CB minimum.

## ■ CONCLUSIONS

A new compound, $Sr_3BeB_6O_{13}$, was discovered in the SrO/BeO/$B_2O_3$ ternary system. This compound crystallizes in the orthorhombic system in centrosymmetric space group *Pnma*. The basic building block of the framework is the novel tri-six-membered ring $[BeB_6O_{13}]^{6-}$, which was found for the first time in the borates. These six-membered rings make up the infinite two-dimensional layers, and between them, the $Sr^{2+}$ cations are filled in. The crystal exhibits inherent incongruent melting, and the UV cutoff edge is below 200 nm. The first-principles studies


dx.doi.org/10.1021/ic400515m | *Inorg. Chem.* 2013, 52, 6136−6141

reveal that the energy band gap of $Sr_3BeB_6O_{13}$ is 7.03 eV (~175 nm), so this crystal might serve as a deep-UV optical material. Further investigation of the growth of large crystals and related physical properties is underway.

## ■ ASSOCIATED CONTENT

### Supporting Information

Coordination environment of $Sr^{2+}$, interatomic distances and angles of $Sr_3BeB_6O_{13}$, a detailed IR spectrum, and band structure and crystal data (CIF) for $Sr_3BeB_6O_{13}$. This material is available free of charge via the Internet at http://pubs.acs.org.

## ■ AUTHOR INFORMATION


### Corresponding Author

*E-mail: zslin@ipc.ac.cn. Telephone: (86)010-82543718. Fax: (86)010-82543709.


### Notes

The authors declare no competing financial interest.

## ■ ACKNOWLEDGMENTS

This work was supported by the National Natural Science Foundation of China (Grants 11174297 and 91022036) and the National Basic Research Project of China (2010CB630701 and 2011CB922204).

## ■ REFERENCES


(1) Becker, P. *Adv. Mater.* **1998**, *10*, 979−992. Kiss, T.; Kanetaka, F.; Yokoya, T.; Shimojima, T.; Kanai, K.; Shin, S.; Onuki, Y.; Togashi, T.; Zhang, C.; Chen, C. T.; Watanabe, S. *Phys. Rev. Lett.* **2005**, *94*, 057001.

(2) Li, R. K.; Ma, Y. Y. *CrystEngComm.* **2012**, *14*, 5421−5424.

(3) Yamada, A.; Iwane, N.; Harada, Y.; Nishimura, S.; Koyama, Y.; Tanaka, I. *Adv. Mater.* **2010**, *22*, 3583−3587. Cakmak, G.; Nuss, J.; Jansen, M. *Z. Anorg. Allg. Chem.* **2009**, *635*, 631.

(4) Chen, C. T.; Wu, B. C.; Jiang, A. D.; You, G. M. *Sci. China, Ser. B: Chem., Life Sci., Earth Sci.* **1985**, *28*, 235.

(5) Chen, C. T.; Wu, Y. C.; Jiang, A. D.; Wu, B. C.; You, G.; Li, R. K.; Lin, S. J. *J. Opt. Soc. Am. B* **1989**, *6*, 616.

(6) Wu, H. P.; Pan, S. L.; Poeppelmeier, K. R.; Li, H. Y.-i.; Jia, D. Z.; Chen, Z. H.; Fan, X. Y.; Yang, Y.; Rondinelli, J. M.; Luo, H. S. *J. Am. Chem. Soc.* **2011**, *133*, 7786−7790.

(7) Wu, H. P.; Yu, H. W.; Yang, Z. H.; Hou, X. L.; Su, X.; Pan, S. L.; Poeppelmeier, K. R.; Rondinelli., J. M. *J. Am. Chem. Soc.* **2013**, *135*, 4215. Wu, H. P.; Yu, H. W.; Yang, Z. H.; Pan, S. L.; Huang, Z. J.; Su, X.; Poeppelmeier, K. R. *Angew. Chem., Int. Ed.* **2013**, *52*, 3406. Yu, H. W.; Wu, H. P.; Pan, S. L.; Yang, Z. H.; Su, X.; Zhang., F. F. *J. Mater. Chem.* **2012**, *22*, 9665.

(8) Mu, R.; Fu, Q.; Jin, L.; Yu, L.; Fang, G.; Tan, D.; Bao, X. *Angew. Chem., Int. Ed.* **2012**, *51*, 4856−4859.

(9) Xu, Y. M.; Richard, P.; Nakayama, K.; Kawahara, T.; Sekiba, Y.; Qian, T.; Neupane, M.; Souma, S.; Sato, T.; Takahashi, T.; Luo, H.-Q.; Wen, H.-H.; Chen, G.-F.; Wang, N.-L.; Wang, Z.; Fang, Z.; Dai, X.; Ding, H. *Nat. Commun.* **2011**, *2*, 392.

(10) Xu, Y. M.; Huang, Y.-B.; Cui, X.-Y.; Razzoli, E.; Radovic, M.; Shi, M.; Chen, G.-F.; Zheng, P.; Wang, N.-L.; Zhang, C.-L.; Dai, P.-C.; Hu, J.-P.; Wang, Z.; Ding, H. *Nat. Phys.* **2011**, *7*, 198−202.

(11) Chen, C. T. *Sci. Sin.* **1979**, *22*, 756. Li, R. K. *J. Non-Cryst. Solids* **1989**, *111*, 199. Chen, C. T.; Wu, Y. C.; Li, R. K. *Int. Rev. Phys. Chem.* **1989**, *8*, 65.

(12) Chen, C. T.; Wang, G. L.; Wang, X. Y.; Xu, Z. Y. *Appl. Phys. B: Lasers Opt.* **2009**, *97*, 9.

(13) Wang, S. C.; Ye, N.; Li, W.; Zhao, D. *J. Am. Chem. Soc.* **2010**, *132*, 8779.

(14) Schaffers, K. I.; Keszler, D. A. *J. Solid State Chem.* **1990**, *85*, 270−274.

(15) Chen, C. T.; Wang, Y. B.; Wu, B. C.; Wu, K.; Zeng, W. L.; Yu, L. H. *Nature* **1995**, *373*, 322.

(16) Sheldrick, G. M. *SHELXS-97, Program for X-ray Crystal Structure Solution*; University of Gottingen: Gottingen, Germany, 1997.

(17) Clark, S. J.; Segall, M. D.; Pickard, C. J.; Hasnip, P. J.; Probert, M. J.; Refson, K.; Payne, M. C. *Z. Krystallogr.* **2005**, *220*, 567.

(18) Kohn, W.; Sham, L. J. *Phys. Rev.* **1965**, *140* (4A), 113.

(19) Lin, J. S.; Qtseish, A.; Payne, M. C.; Heine, V. *Phys. Rev. B* **1993**, *47*, 4174.

(20) Kleinman, L.; Bylander, D. M. *Phys. Rev. Lett.* **1982**, *48*, 1425−1428.

(21) Monkhorst, H. J.; Pack, J. D. *Phys. Rev. B* **1976**, *13*, 5188−5192.

(22) Lin, Z. S.; Kang, L.; Zheng, T.; He, R.; Chen, C. T. *Comput. Mater. Sci.* **2012**, *60*, 99.

(23) Adamo, C.; Barony, V. *J. Chem. Phys.* **1998**, *110*, 6158−6170.

(24) Perdew, J. P.; Burke, K.; Ernzerhof, M. *Phys. Rev. Lett.* **1996**, *77* (18), 3865−3868.

(25) Godby, R. W; Schluter, M.; Sham, L. J. *Phys. Rev. B* **1988**, *37*, 10159. Wang, C. S.; Klein, B. M. *Phys. Rev. B* **1981**, *24*, 3417.

(26) Chen, C. T.; Wang, Y. B.; Xia, Y. N.; Wu, B. C.; Tang, D. Y.; Wu, K. C.; Zeng, W. R.; Yu, L. H. *J. Appl. Phys.* **1995**, *77*, 2268. Wang, S. C.; Ye, N.; Li, W.; Zhao, D. *J. Am. Chem. Soc.* **2010**, *132*, 8779. Huang, H. W.; Yao, J. Y.; Lin, Z. H.; Wang, X. Y.; He, R.; Yao, W. J.; Zhai, N. X.; Chen, C. T. *Angew. Chem., Int. Ed.* **2011**, *50*, 9141. Huang, H. W.; Yao, J. Y.; Lin, Z. H.; Wang, X. Y.; He, R.; Yao, W. J.; Zhai, N. X.; Chen, C. T. *Chem. Mater.* **2011**, *23*, 5457.

(27) Meng, X. Y. Ab-initio Studies of the Polymorphous Problem of Structure in SBBO ($Sr_2Be_2B_2O_7$) Family Nonlinear Optical Crystals and Mechanism of the Electro-Optic Effect in Perovskite-Type Ferroelectrics. Ph.D. Dissertation, Technical Institute of Physics and Chemistry, Chinese Academy of Science, Beijing, 2006.

(28) Cong, R.; Sun, J. L.; Yang, T.; Li, M. R.; Liao, F. H.; Wang, Y. X.; Lin, J. H. *Inorg. Chem.* **2011**, *50*, 5098. Fan, X. Y.; Pan, S. L.; Hou, X. L.; Tian, X. L.; Han, J.; Haag, J.; Poeppelmeier, K. R. *Cryst. Growth Des.* **2010**, *10*, 252. Yang, Y.; Pan, S. L.; Hou, X. L.; Dong, X. Y.; Su, X.; Yang, Z. H.; Zhang, M.; Zhao, W. W.; Chen, Z. H. *CrystEngComm* **2012**, *14*, 6720−6725.

(29) Korotkov, A. S.; Atuchin, V. V. *Opt. Commun.* **2008**, *281*, 2132−2138.